

# Space charge effects on mass accuracy for multiply charged ions in ESI–FTICR

P. Kristina Taylor, I. Jonathan Amster\*

*Department of Chemistry, University of Georgia, Athens, GA 30602, USA*

Received 6 May 2002; accepted 18 September 2002

## Abstract

Ion space charge causes systematic shifts in the observed cyclotron frequencies of ions, limiting accurate mass measurements in Fourier transform ion cyclotron resonance (FTICR). Presented here are studies of space charge effects on mass accuracy for multiply charged ions produced by electrospray ionization. Axialization of the ion cloud by quadrupolar excitation increases space charge-induced shifts in observed frequency but reduces the random errors in measurements by distributing ions in the analyzer cell in a reproducible manner. Space charge-induced shifts in observed frequency are observed to be independent of charge state. Because all ions experience the same space charge-induced frequency shift, internal calibration is accurate without regard to differences between the charge states of the calibrant and analyte peaks. Space charge-induced frequency shifts in externally calibrated mass spectra can be corrected to provide significant improvement in mass accuracy for such measurements. (*Int J Mass Spectrom* 222 (2003) 351–361)

© 2002 Elsevier Science B.V. All rights reserved.

*Keywords:* Electrospray ionization; Ion cyclotron resonance; Proteins

## 1. Introduction

Fourier transform ion cyclotron resonance (FTICR) mass spectrometry is a technique known for its high mass resolution and mass accuracy. These features enhance a wide variety of mass spectrometric studies, including polymer analysis [1–6], oxidation state studies of metalloproteins [7,8], high throughput proteomics and database searching [9–20], and protein sequencing [21–24]. Space charge effects have long been known to limit mass accuracy measurements in ICR and FTICR mass spectrometry [25,26]. Space charge arises from the influence of the electric field of ions in the trapped analyzer cell upon each other, and

it has been quantified in the equation for the observed frequency of motion of ions in a magnetic field developed by Jeffries, Barlow, and Dunn, and refined by McIver and coworkers, Eq. (1) [27,28]. The first term in the right side of the equation is the unperturbed cyclotron frequency, where  $q$  is the coulombic charge on the ion,  $B$  is the strength of the magnetic field, and  $m$  is the mass of the ion. The second term is equal to the magnetron frequency of the ions, produced by the influence of the voltage used to trap the ions within the cell, where  $a$  is the diameter of the cell,  $\alpha$  is a constant determined by the cell geometry, and  $V$  is the voltage applied to the trap plates. The third term quantifies the space charge effect on observed frequency, where  $\rho$  is the ion density,  $G_i$  is a constant that is related to the geometry of the ion cloud, and  $\epsilon_0$  is the permittivity

\* Corresponding author. E-mail: jamster@uga.edu

of free space. The greatest variation in the magnitude of the space charge effect arises from differences in ion density, caused by changes in the number of ions within the cell from one ionization event to the next. Unless space charge is either taken into account or eliminated, high mass accuracy measurements cannot be reliably achieved. This is particularly true for matrix-assisted laser desorption/ionization (MALDI) experiments due to the large shot-to-shot variation in ion yield. A recent study of MALDI–FTICR showed space charge-induced variations in measured mass of 50–100 ppm in a 4.7 T instrument [2].

$$\omega_{\text{obs}} = \frac{qB}{m} - \frac{2\alpha V}{a^2 B} - \frac{q\rho G_i}{\epsilon_0 B} \quad (1)$$

A number of valuable efforts have been made to study and quantitate space charge effects on mass accuracy for singly charged ions [2,25,27–36]. Jeffries et al. presented a mathematical treatment of space charge in the scanning ICR experiment [27]. McIver and coworkers based their equation for space charge (Eq. (1)) on Jeffries' work [28]. Chen and coworkers have examined space charge by representing rotating ions as a pair of points, line charges, or cylinders [29,30]. Recently, Easterling et al. have examined space charge-induced shifts in observed frequency for high mass ions formed by MALDI [2]. Smith and coworkers have developed a deconvolution routine known as DeCAL which systematically removes the space charge-induced frequency shifts in mass spectra of multiply-charged ions [37]. Further efforts have been made to reduce or negate the effects of space charge through physical means [38–43]. Increasing the magnetic field strength decreases the magnitude of space charge effects, among other benefits [44,45]. A more general approach involves the manipulation of the ion population within the cell, typically through variation of the ICR pulse sequence. The trap plates may be momentarily grounded, suspended trapping [41], or an asymmetric trap plate voltage can be applied to reduce the number of ions in the cell. The smaller number of ions trapped in this manner greatly reduces the effects of space charge. A third method for reducing the effect of space charge on mass accu-

racy is to use an internal calibrant [43,44,46,47], as the calibrant is subjected to the same frequency shift as the species of interest. Eq. (1) suggests that space charge-induced frequency shifts are proportional to the charge on an ion, and that multiply-charged ions should exhibit proportionally larger shifts than their singly-charged counterparts. If this is true, then one would need to take charge state into account even when performing internal calibration. Furthermore, it is often impractical to use an internal standard with electrospray ionization, as mixtures are susceptible to suppression effects that can favor the production of one ionic species over others. In such a case, external calibration must be used. For external calibration in ESI–FTICR, it is necessary to have a quantitative understanding of space charge effects on mass accuracy in order to compensate for differences in ion population between the analyte and the calibrant mass spectra. The recently published DeCAL method for compensating for space charge effects relies on knowing the relationship between charge state and frequency shift [37]. For all these reasons, it is important to characterize the effect of ion population and charge state on observed frequency, in order to achieve high mass accuracy. Here we use electrospray ionization FTICR to examine space charge-induced frequency shifts for multiply charged ions and discern the effect of charge state on mass accuracy.

## 2. Experimental

Melittin (MW = 2863 Da), insulin (bovine, MW = 5733 Da), ubiquitin (bovine, MW = 8565 Da), hemoglobin (bovine, MW for A-chain = 15,053 Da, for B-chain = 15,954 Da), insulin chain B (bovine, MW = 3497 Da), and myoglobin (equine, MW = 16,951 Da) were purchased from Sigma (St. Louis, MO) and used without further purification. All samples were dissolved in a solution of 49:49:2 water:methanol:acetic acid (v/v) to a concentration of 10  $\mu\text{M}$ . Internal calibration experiments were performed by mixing 30  $\mu\text{L}$  of hemoglobin with 30  $\mu\text{L}$  of insulin chain B. Ions were produced via nanospray

through tips fabricated in-house from 100  $\mu\text{m}$  i.d. fused silica (Supelco, Bellefonte, PA) [48]. Sample solutions were introduced to the spray tips with a syringe pump operated at a flow rate of 6  $\mu\text{L}/\text{h}$ . Approximately 1.2 kV was applied to the needle of the syringe, which forms a liquid junction with the emitter tip.

Mass spectrometry was performed with a Bruker BioApex 7 T FTICR mass spectrometer equipped with an Analytica source which has been modified by replacing the glass capillary with a heated metal capillary interface [8]. The heated metal capillary was maintained at a temperature of 150 °C. Quadrupolar excitation (QE) [49,50] was performed with nitrogen as the collision gas for all samples. The gas pulse was applied for 4 s, raising the pressure in the analyzer between  $6 \times 10^{-5}$  and  $2 \times 10^{-4}$  Torr, and the QE pulse was initiated simultaneously. QE was continued at 35.7  $V_{\text{p-p}}$  for 6 s after closing the pulse valve, until the pressure in the analyzer reached  $1 \times 10^{-7}$  Torr. A subsequent 30 s pumpdown delay allowed pressure in the analyzer to reach  $1\text{--}2 \times 10^{-8}$  Torr, at which time the ions were excited and detected. These QE conditions were optimized to produce remeasurement efficiencies over 99% [49,51]. For the space charge experiments utilizing QE, a packet of ions was produced and guided into the cell through a series of electrostatic lenses. QE was used to center the ions, and a single scan was acquired. The ionization pulse was turned off, and two more single scans were obtained using QE to remeasure the original ion packet. In this manner, three separate measurements were made for the same population of ions. A 50  $\mu\text{s}$  cell quench pulse was then applied to the trap plates to remove approximately 10% of the ions from the cell. QE and remeasurement were then used to acquire three more mass spectra of the remaining ion population. The sequence of partial cell quench followed by three acquisitions was repeated until the signal had either decreased by an order of magnitude or was undetectable.

The experiments done without QE and without collision gas were performed by optimizing the signal intensity and then acquiring three mass spectra, each with a separate ionization pulse. The length of the ionization pulse was then decreased slightly (500  $\mu\text{s}$ ) to

reduce the signal intensity, and three more mass spectra were acquired. This procedure was repeated until the signal was undetectable. The experiments done without QE but with a gas pulse were performed in the same fashion, except that a 4 s gas pulse and a 30 s pump down delay were included prior to excitation/detection. The ubiquitin and insulin spectra used to demonstrate space charge correction were obtained using identical pulse sequences. Four ionization pulses were interspersed with two 1.5 s gas pulses. A 90 s delay to pump away the gas was followed by excitation/detection. The front and rear trap plates were held at 0.5 and 0.65 V, respectively.

### 3. Results and discussion

Ions produced by electrospray ionization exhibit systematic shifts in their observed frequency that correlate with the number of ions in the cell. Fig. 1 shows mass spectra for the 3+ charge state of insulin exhibiting a frequency shift that correlates with signal intensity. For these experiments, the ions were axialized by QE prior to detection. Fig. 1a shows insulin at full intensity; Fig. 1b shows the same ion packet, after a series of remeasurements and short cell quenches, at 60% of its original intensity; and Fig. 1c shows the same ion packet at 25% of its original intensity. The mass-to-charge ( $m/z$ ) ratio of the peaks are observed to systematically shift to lower values (higher frequency) as the total ion intensity decreases, in qualitative agreement with Eq. (1). The frequency shift between the peaks in Fig. 1a and c is 2.5 Hz, or 43 ppm. Clearly, calibration with the top mass spectrum would lead to unacceptably large errors if applied to a mass spectrum with a total ion intensity as in the bottom mass spectrum.

Previous research using a 4.7 T MALDI-FTICR mass spectrometer with an open-ended cylindrical analyzer cell has shown that the magnitude of random errors in frequency measurement depend on the manner in which the ion cloud is treated prior to excitation and detection [2]. The largest errors were observed when the ions experienced no collisional damping of

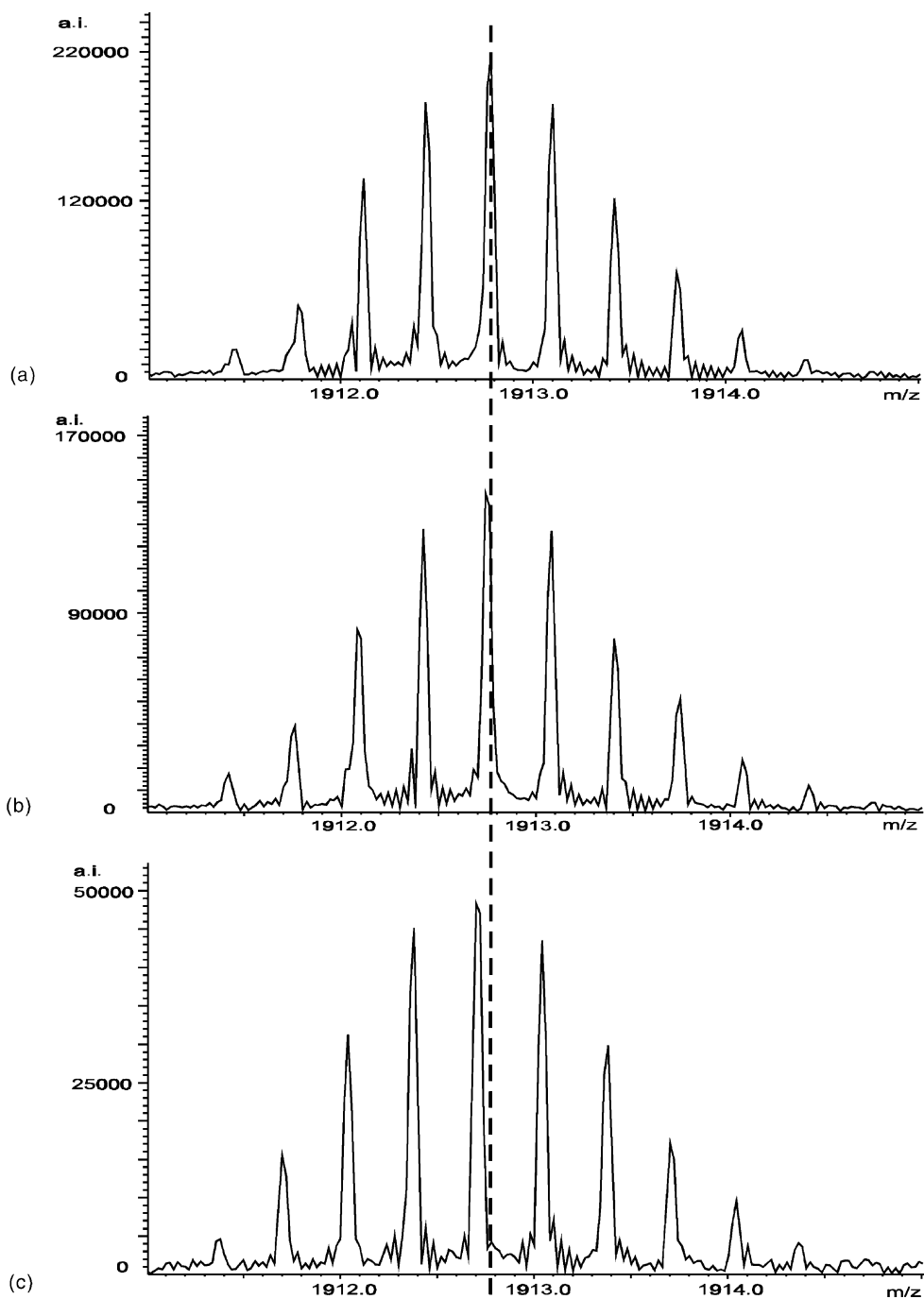


Fig. 1. ESI-FTICR mass spectra of insulin, using quadrupolar excitation to isolate the 3+ charge state and short cell quenches to systematically reduce ion density, exhibiting a frequency shift. (a) The 3+ charge state of insulin at full intensity. (b) The same ion packet after repeated quadrupolar excitation and short cell quenches, at 60% of the full intensity. (c) The same ion packet at 25% of the full intensity. The dashed line bisecting the base peak in (a) is meant to guide the eye in observing the space charge-induced frequency shift.

their axial motion, and the least when the ions were subjected to quadrupolar excitation prior to detection. This result is also observed in these experiments, obtained with a 7 T ESI–FTICR mass spectrometer with a cylindrical analyzer cell with Infinity trapping plates, as shown in Fig. 2. Fig. 2a shows a plot of the observed frequency shift vs. total signal intensity for the 4+ charge state of insulin, with no collisional quenching of the ions prior to detection. The mea-

sured property of signal intensity correlates to the ion density term of Eq. (1), as image current is directly proportional to the amount of charge being detected. The scatter observed in the plot is greater than that observed in the other two experiments, and indicates fluctuations in the ion density, as ions assume different distributions along the central axis of the cell prior to the excite pulse. Fig. 2b shows a plot of observed frequency vs. signal intensity for the 3+ charge state

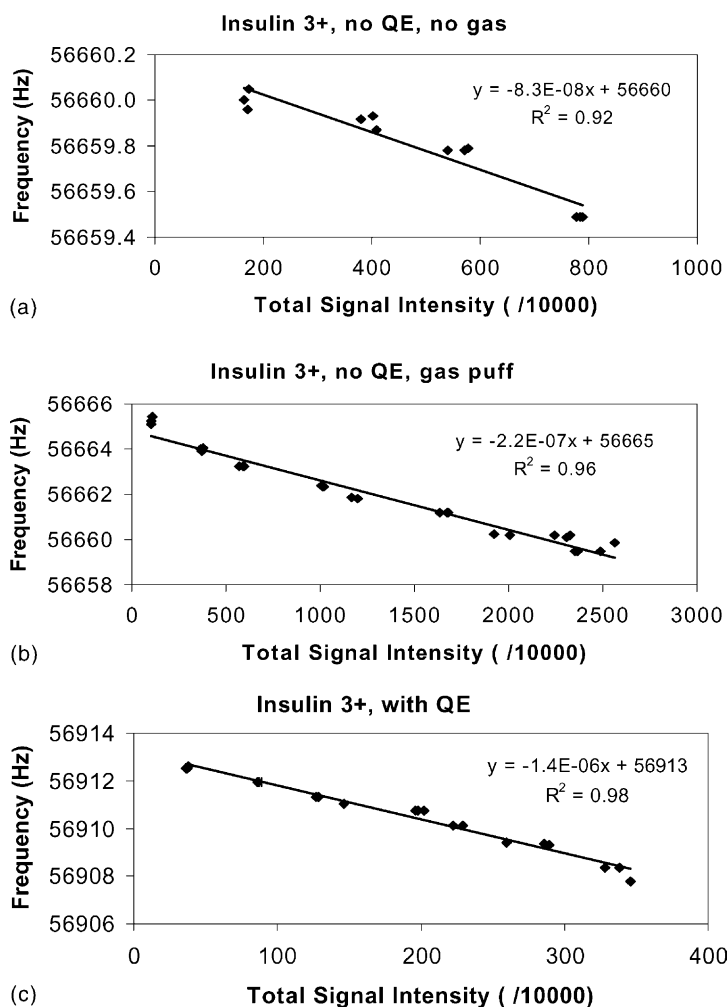


Fig. 2. Plots of signal intensity vs. frequency for the monoisotopic peak of the 3+ charge state of insulin under various conditions of axial cooling. (a) Insulin with no gas pulse, exhibiting the largest observed scatter. (b) Insulin with a short gas pulse to damp axial motion through collisions. Less scatter is observed in the plot, as evidenced by the higher  $R^2$  correlation constant. The slope of this plot is almost three times as steep as that of (a), indicating an increase in space charge. (c) Insulin with QE applied to axialize the ions. This plot shows the smallest amount of scatter and the largest space charge effects.

of insulin when a short nitrogen gas pulse was introduced just after ions were injected into the cell. This gas pulse provides collisional damping of the axial ion motion, reducing the distribution of the ions along the magnetic field axis within the cell. This creates a more reproducible ion distribution, leading to a reduction in the amount of scatter in the plot relative to Fig. 2a. Fig. 2c shows a plot of frequency vs. signal intensity for the 3+ charge state of insulin with a QE pulse applied. The QE pulse was used to center (axialize) the ions within the cell and reduce their magnetron motion, creating the most reproducible ion distribution between experiments, yielding a plot with the least amount of scatter.

The magnitude of the space charge effect is also influenced by the compression of the ion cloud from collisional damping and quadrupolar excitation, as can be seen from the change in slopes of Fig. 2a–c. The slopes of these plots are a measure of the space charge-induced frequency shifts. The smallest slope, denoting the least change in frequency and the smallest space charge effect, is found when the ions experience no collisional damping (Fig. 2a). The greatest effect is seen when QE is applied (Fig. 2c), as a result of the high ion density created when the ions are squeezed into the center of the FTICR analyzer cell. In order to reduce random errors in mass measurement, we chose to utilize QE, despite the more pronounced space charge effect and its concomitant larger systematic error.

According to the space charge term in the observed frequency equation developed by Jeffries et al. [27], and McIver and coworkers [28], the decrease in observed frequency attributed to the space charge effect should scale with the number of charges on the ion, Eq. (1). For example, a doubly-charged ion should experience twice the space charge-induced frequency shift of a singly-charged ion, a triply-charged ion should experience three times the shift, etc. The slopes of the plots of observed frequency vs. signal intensity for ions of charge states from 1+ to 8+ is shown in Table 1. As mentioned above, the signal intensity is proportional to both the number of charges on an ion and the number of ions measured. A given

Table 1

Measured slopes and intercepts for plots of observed frequency vs. total ion intensity for ions with charge states from 1+ to 8+

Protein	Charge state	Slope	Intercept (Hz)
Melittin	1+	$-9.9 \times 10^{-7}$	38217
Melittin	2+	$-1.1 \times 10^{-6}$	76423
Insulin	3+	$-1.4 \times 10^{-6}$	56913
Ubiquitin	6+	$-1.1 \times 10^{-6}$	76180
Myoglobin	8+	$-1.2 \times 10^{-6}$	49310

number of doubly-charged ions will produce a peak with twice the intensity than that from the same number of singly charged ions. For these experiments, total signal intensity was calculated by summing the individual peak intensities. This value correlates to *charge* density rather than *ion* density. The frequency of a selected peak was monitored as the total signal intensity was varied systematically. As can be seen in Table 1, there is no systematic increase in space charge effect with increasing charge state, in contradiction to the term for space charge effect in Eq. (1). There are variations in the slopes of the plots ( $\pm 18\%$ ), but these variations do not appear to correlate with the charge state of the ion. Two possible explanations for these variations can be postulated. First, there may be a higher-order term for space charge in the equation for observed frequency, Eq. (1). A more likely possibility is that the variations may be caused by experimental parameters that are difficult to control. For example, the pulsed introduction of gas for collisional damping is unlikely to produce an identical pressure each time, leading to slightly different ion spatial distributions from experiment to experiment.

To reduce the experimental errors in the slopes of the space charge plots, a series of measurements was performed on ions of differing charge states present in the cell at the same time. In this manner, all ions experience identical experiment-to-experiment variations in the parameters that are difficult to control. A short gas pulse was applied to dampen the axial motion of the ions and reduce the amount of scatter in the plots rather than using QE to axialize ions. Plots of frequency vs. signal intensity for ubiquitin and cytochrome *c* are shown in Fig. 3a–d. Fig. 3a shows

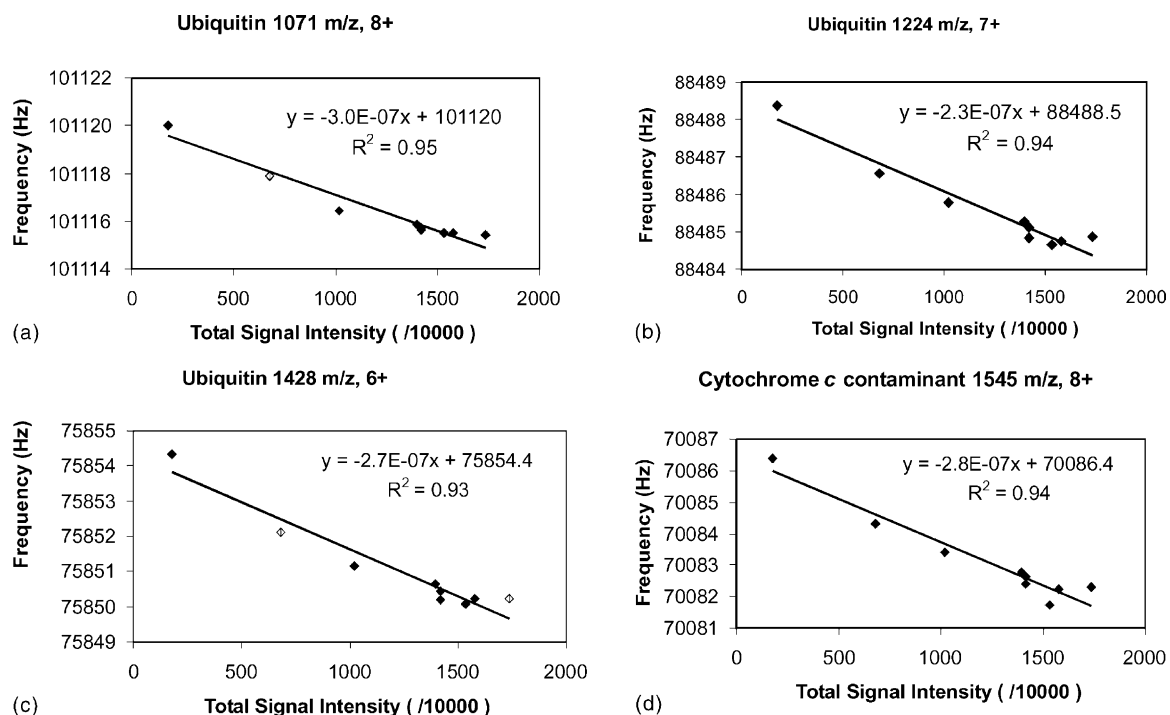


Fig. 3. Plots of frequency vs. signal intensity for a range of charge states monitored simultaneously as a function of ion intensity, using a gas pulse to damp the axial motion of the ions. The ion density was varied by detuning the skimmer potential. (a) Ubiquitin 8+ charge state, at  $m/z$  1071. (b) Ubiquitin 7+ charge state, at  $m/z$  1224. (c) Ubiquitin 6+ charge state, at  $m/z$  1428. (d) Cytochrome *c* (contaminant), 8+ charge state, at  $m/z$  1545.

the 8+ charge state of ubiquitin at  $m/z$  1071, Fig. 3b shows the 7+ charge state at  $m/z$  1224, Fig. 3c shows the 6+ charge state at  $m/z$  1428, and Fig. 3d shows the 8+ charge state of a cytochrome *c* component at  $m/z$  1545. A close examination of the data shows that the residual errors, that is, the deviation of individual measurements from the least squares fitted line, is the same for all the different ions at each intensity measurement. This shows that there is some variability due to random error between measurements, but that in a given measurement, all ions are experiencing the same conditions. The slopes of the plots for the ions at  $m/z$  1071, 1428, and 1545 lie within the range of  $-2.8 \times 10^{-7} \pm 7\%$ . The relative standard deviation in the slopes of these lines is 8%, and so we conclude that the slopes of the plots in Fig. 3a, c and d are the same within experimental error. The slope of the plot for the ion of  $m/z$  1224 is  $-2.3 \times 10^{-7}$  (Fig. 3b) and is smaller than

the other measurements by 18%, an amount roughly equal to two standard deviations. Thus, a small but statistically significant difference is observed in the slope of the space charge plot for this ion. We can only speculate on the nature of this small difference. One possibility is that the space charge-induced shift may have a weak dependence on the relative abundance of the ions. Fig. 4 shows a representative mass spectrum from the series of measurements. As can be seen, the  $m/z$  1224 ion, which had the lowest slope in its space charge plot, is by far the most abundant ion in the mass spectrum. In a previous study of space charge effects on mass accuracy for singly-charged ions, it was found that the frequency shifts of all ions were the same, and independent of their relative abundance, and so such an effect, if present for multiply-charged ions, would be surprising. It should be noted that the difference in the slope is small (a factor of 2 larger

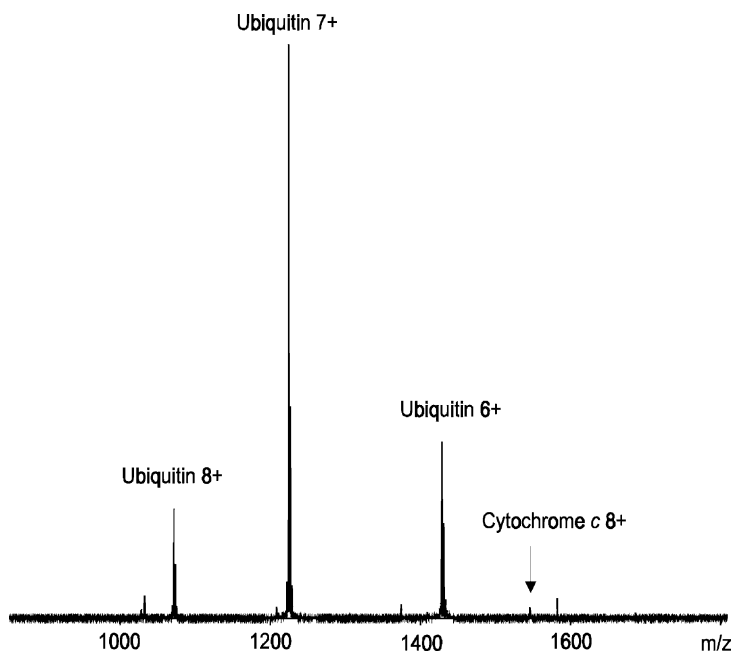


Fig. 4. Sample mass spectrum of a range of charge states monitored simultaneously as a function of ion intensity, showing the relative abundance of each species in the cell.

than the standard deviation in the measurement), and that this effect is a small perturbation to the general observation that all slopes are the same. The very low abundance cytochrome *c* ion at  $m/z$  1545 (<3% relative abundance) exhibits the same slope as the ions of 20–30% relative abundance, and only the most abundant peak exhibits a smaller slope. Some space charge behaviors have been reported that are sensitive to relative abundance. For example, the loss of coherence of an orbiting ion cloud through coulombic interactions with other ion clouds, dubbed ion cloud shearing, is known to effect low abundance ions more profoundly than higher abundance ions [52]. Further studies will be required to determine if the small but perceptible difference in the slope of the space charge plots is related to the abundance of the ions.

Since there appears to be no effect on the magnitude of the space charge-induced frequency shifts with variation in charge state, it is possible to calibrate using two peaks which bracket the peak of interest without regard for their charge state. Table 2 shows the

data for the 8+ to 13+ charge states of hemoglobin chain A, calibrated internally with the 2+ ( $m/z$  1748) and 3+ ( $m/z$  1166) charge states of insulin chain B. The mass errors are small, approximately 1 ppm for interpolated values, 6 ppm for an extrapolated value. Internal calibration is successful because the space charge-induced frequency shift is not dependent on charge state, and because the calibrant and analyte peaks experience the same total ion density and

Table 2

Experimentally determined monoisotopic mass and error for internally calibrated ions with charge states from 8+ to 13+

$m/z$	Charge state	Experimental MI mass (Da)	Theoretical MI mass (Da)	Error (ppm)
1158	13+	15043.99	15043.90	6.0
1255	12+	15043.92	15043.90	1.3
1369	11+	15043.92	15043.90	1.3
1506	10+	15043.88	15043.90	1.3
1673	9+	15043.90	15043.90	<1.0
1882	8+	15043.90	15043.90	<1.0

Table 3

Monoisotopic mass values derived from the 3+ to 5+ charge states of insulin, before and after correction for space charge

<i>m/z</i>	Charge state	Calculated MI mass (Da)	Externally calibrated MI mass (Da)	Error (ppm)	Adjusted MI mass (Da)	Error (ppm)
956	6+	5729.600	5729.672	12.5	5729.607	1.1
1146	5+	5729.600	5729.687	15.1	5729.608	1.3
1433	4+	5729.600	5729.698	17.1	5729.600	−0.1
1910	3+	5729.600	5729.702	17.7	5729.577	−4.0

Errors are calculated from the theoretical monoisotopic mass of 5729.600.

therefore the same space charge-induced frequency shift.

Internal calibration is sometimes difficult to implement. For example, an online LC/ESI–MS experiment would require a second, concurrent method of sample introduction for the calibrant. External calibration introduces a systematic error due to differences in ion population between calibrant and analyte, but these effects can be accounted for using Eq. (2), developed by Easterling et al. [2], where  $f_{\text{estimated}}$  is the frequency after adjustment for space charge,  $f_{\text{measured}}$  is the frequency obtained with external calibration,  $c$  is the slope of the frequency vs. ion intensity plot,  $I_{\text{calibrant}}$  is the total ion intensity of the calibrant, and  $I_{\text{analyte}}$  is the total ion intensity of the analyte. Table 3 shows externally calibrated monoisotopic masses and errors for four charge states of insulin calibrated with ubiquitin, as well as monoisotopic masses and errors after correction for space charge. The ubiquitin calibrant spectrum and insulin analyte spectrum were obtained using the same conditions, and the intensities were obtained by summing the intensities of the individual isotope peaks. The slope used for space charge correction was  $-2.7 \times 10^{-7}$ , obtained from the frequency vs. intensity plot of ubiquitin *m/z* 1428, without QE. The errors prior to adjustment for space charge range from 13 to 18 ppm. These errors are relatively small, even without correcting for space charge, because QE was not used in this experiment, reducing the density of the ion distribution. Nevertheless, correcting for space charge-induced frequency shifts using Eq. (2) reduces the error by an order of magnitude, from an average of 16 to 1.6 ppm. Clearly, accounting for space charge in this manner increases the level of

mass accuracy. We have attempted to apply the procedure of external calibration followed by correction for space charge to larger biological molecules, but it has proven less successful. As the size of the molecule and number of charge states in the spectrum increases, the pattern of constructive/destructive interference in the transient becomes more complex [53,54]. This complexity affects the magnitude of the spectral peaks, so that the total signal intensity obtained by summing the intensities of the individual isotope peaks is not truly representative of the total ion density within the cell [53]. The procedure of internal calibration works well for these larger molecules. As shown in Table 2, ions with 13+ charges can be calibrated using ions with 2+ to 3+ charges, while still achieving low ppm mass accuracy.

$$f_{\text{estimated}} = f_{\text{measured}} + c(I_{\text{calibrant}} - I_{\text{analyte}}) \quad (2)$$

#### 4. Conclusions

Space charge produces a shift in observed frequency with variations in ion density, limiting mass accuracy. Prior research on singly charged ions produced by MALDI has shown a reduction in random error in measurements of cyclotron frequency when ion motion is collisionally damped [2]. This finding has proven to be equally valid for multiply charged ions produced by ESI. On the other hand, the space charge effect is more significant when the ion cloud is more compressed, e.g., by collisional damping of axial motion or by quadrupolar excitation. Therefore, the same techniques commonly used to produce better signal can reduce mass accuracy by increasing space

charge. However, the space charge-induced frequency shift is a systematic error, and can be treated through proper calibration. Space charge-induced frequency shifts do not change with increasing charge on the ion, in contrast to expectations based on Eq. (1). Significantly, the space charge-induced frequency shifts are the same for a distribution of ions with various charge states when they are monitored simultaneously. Thus, it is possible to achieve high mass accuracy of one ion species through internal calibration without regard for the charge state of either the calibrant or the analyte peaks. External calibration can be improved by the use of a correction factor for space charge. If the total ion intensities of the analyte and calibrant peaks can be accurately determined, a frequency correction factor based on the slope of a frequency vs. total ion intensity plot for the calibrant can greatly improve mass accuracy. As the mass of the analyte and range of charge states increases, the determination of the total ion intensity by summation of the individual peak intensities becomes problematic, reducing the accuracy of external calibration. The best mass accuracy for high mass species is achieved when the mass of the calibrant and analyte are comparable.

## Acknowledgements

The authors are grateful for generous financial support from NSF (CHE-9974579).

## References

- [1] E.P. Maziarz, G.A. Baker, T.D. Wood, *Macromolecules* 32 (1999) 4411.
- [2] M.L. Easterling, T.H. Mize, I.J. Amster, *Anal. Chem.* 71 (1999) 624.
- [3] M.L. Easterling, T.H. Mize, I.J. Amster, *Int. J. Mass Spectrom. Ion Process.* 169 (1997) 387.
- [4] R.M.A. Heeren, C.G. Dekoster, J.J. Boon, *Anal. Chem.* 67 (1995) 3965.
- [5] C.G. Dekoster, M.C. Duursma, G.J. Vanrooij, R.M.A. Heeren, J.J. Boon, *Rapid Commun. Mass Spectrom.* 9 (1995) 957.
- [6] M. Dey, J.A. Castoro, C.L. Wilkins, *Anal. Chem.* 67 (1995) 1575.
- [7] F. He, C.L. Hendrickson, A.G. Marshall, *J. Am. Soc. Mass Spectrom.* 11 (2000) 120.
- [8] K. Johnson, M. Verhagen, P. Brereton, M. Adams, I. Amster, *Anal. Chem.* 72 (2000) 1410.
- [9] J.J. Li, J.F. Kelly, I. Chemushevich, D.J. Harrison, P. Thibault, *Anal. Chem.* 72 (2000) 599.
- [10] C. Borchers, J.F. Peter, M.C. Hall, T.A. Kunkel, K.B. Tomer, *Anal. Chem.* 72 (2000) 1163.
- [11] M.T. Davis, T.D. Lee, *J. Am. Soc. Mass Spectrom.* 9 (1998) 194.
- [12] T. Kosaka, T. Takazawa, T. Nakamura, *Anal. Chem.* 72 (2000) 1179.
- [13] J. Eriksson, B.T. Chait, D. Fenyo, *Anal. Chem.* 72 (2000) 999.
- [14] M.K. Green, M.V. Johnston, B.S. Larsen, *Anal. Biochem.* 275 (1999) 39.
- [15] K.R. Clauser, P. Baker, A.L. Burlingame, *Anal. Chem.* 71 (1999) 2871.
- [16] D. Fenyo, J. Qin, B.T. Chait, *Electrophoresis* 19 (1998) 998.
- [17] E.J. Takach, W.M. Hines, D.H. Patterson, P. Juhasz, A.M. Falick, M.L. Vestal, S.A. Martin, *J. Protein Chem.* 16 (1997) 363.
- [18] K.L. Oconnell, J.T. Stults, *Electrophoresis* 18 (1997) 349.
- [19] M. Mann, P. Hojrup, P. Roepstorff, *Biol. Mass Spectrom.* 22 (1993) 338.
- [20] D.R. Goodlett, J.E. Bruce, G.A. Anderson, B. Rist, L. Pasa-Tolic, O. Fiehn, R.D. Smith, R. Aebersold, *Anal. Chem.* 72 (2000) 1112.
- [21] A. Shevchenko, M. Wilm, M. Mann, *J. Protein Chem.* 16 (1997) 481.
- [22] A. Shevchenko, A. Loboda, A. Shevchenko, W. Ens, K. Standing, *Anal. Chem.* 72 (2000) 2132.
- [23] A. Shevchenko, I. Chernushevich, W. Ens, K.G. Standing, B. Thomson, M. Wilm, M. Mann, *Rapid Commun. Mass Spectrom.* 11 (1997) 1015.
- [24] T.I. Stevenson, J.A. Loo, K.D. Greis, *Anal. Biochem.* 262 (1998) 99.
- [25] H. Sommer, H. Thomas, J. Hipple, *Phys. Rev.* 76 (1949) 1877.
- [26] J. Beauchamp, J. Armstrong, *Rev. Sci. Instrum.* 40 (1969) 123.
- [27] J.B. Jeffries, S.E. Barlow, G.H. Dunn, *Int. J. Mass Spectrom. Ion Process.* 54 (1983) 169.
- [28] T.J. Francl, M.G. Sherman, R.L. Hunter, M.J. Locke, W.D. Bowers, R.T. McIver, *Int. J. Mass Spectrom. Ion Process.* 54 (1983) 189.
- [29] S.P. Chen, M.B. Comisarow, *Rapid Commun. Mass Spectrom.* 5 (1991) 450.
- [30] R. Chen, A.G. Marshall, *Int. J. Mass Spectrom. Ion Process.* 133 (1994) 29.
- [31] S.J. Han, S.K. Shin, *J. Am. Soc. Mass Spectrom.* 8 (1997) 319.
- [32] E.B. Ledford, D.L. Rempel, M.L. Gross, *Anal. Chem.* 56 (1984) 2744.
- [33] E.B. Ledford, D.L. Rempel, M.L. Gross, *Int. J. Mass Spectrom. Ion Process.* 55 (1984) 143.
- [34] D.W. Mitchell, R.D. Smith, *Phys. Rev. E* 52 (1995) 4366.

- [35] A.J. Peurrung, R.T. Kouzes, *Int. J. Mass Spectrom. Ion Process.* 145 (1995) 139.
- [36] G.T. Uechi, R.C. Dunbar, *J. Am. Soc. Mass Spectrom.* 3 (1992) 734.
- [37] J.E. Bruce, G.A. Anderson, M.D. Brands, L.P. Tolic, R.D. Smith, *J. Am. Soc. Mass Spectrom.* 11 (2000) 416.
- [38] J.S. Anderson, D.A. Laude, *Int. J. Mass Spectrom. Ion Process.* 158 (1996) 163.
- [39] S.A. Hofstadler, D.A. Laude, *J. Am. Soc. Mass Spectrom.* 3 (1992) 615.
- [40] J.D. Hogan, D.A. Laude, *Anal. Chem.* 62 (1990) 530.
- [41] D.A. Laude, S.C. Beu, *Anal. Chem.* 61 (1989) 2422.
- [42] J.T. Stults, *Anal. Chem.* 69 (1997) 1815.
- [43] R.D. Burton, K.P. Matuszak, C.H. Watson, J.R. Eyler, *J. Am. Soc. Mass Spectrom.* 10 (1999) 1291.
- [44] M.W. Senko, C.L. Hendrickson, L. PasaTolic, J.A. Marto, F.M. White, S.H. Guan, A.G. Marshall, *Rapid Commun. Mass Spectrom.* 10 (1996) 1824.
- [45] M.V. Gorshkov, L.P. Tolic, H.R. Udseth, G.A. Anderson, B.M. Huang, J.E. Bruce, D.C. Prior, S.A. Hofstadler, L.A. Tang, L.Z. Chen, J.A. Willett, A.L. Rockwood, M.S. Sherman, R.D. Smith, *J. Am. Soc. Mass Spectrom.* 9 (1998) 692.
- [46] S.A. Hofstadler, R.H. Griffey, L. Pasa-Tolic, R.D. Smith, *Rapid Commun. Mass Spectrom.* 12 (1998) 1400.
- [47] S.A. Lorenz, M.A. Moy, A.R. Dolan, T.D. Wood, *Rapid Commun. Mass Spectrom.* 13 (1999) 2098.
- [48] M. Wilm, M. Mann, *Anal. Chem.* 68 (1996) 1.
- [49] J.P. Speir, G.S. Gorman, C.C. Pitsenberger, C.A. Turner, P.P. Wang, I.J. Amster, *Anal. Chem.* 65 (1993) 1746.
- [50] L. Schweikhard, S.H. Guan, A.G. Marshall, *Int. J. Mass Spectrom. Ion Process.* 120 (1992) 71.
- [51] V.L. Campbell, Z.Q. Guan, D.A. Laude, *J. Am. Soc. Mass Spectrom.* 6 (1995) 564.
- [52] D.W. Mitchell, R.D. Smith, *Int. J. Mass Spectrom. Ion Process.* 165 (1997) 271.
- [53] M.L. Easterling, I.J. Amster, G.J. van Rooij, R.M.A. Heeren, *J. Am. Soc. Mass Spectrom.* 10 (1999) 1074.
- [54] S.A. Hofstadler, J.E. Bruce, A.L. Rockwood, G.A. Anderson, B.E. Winger, R.D. Smith, *Int. J. Mass Spectrom. Ion Process.* 132 (1994) 109.